

# PAPR Reduction and Performance Improvement in OFDM Systems using WHT-based Schemes

Guilherme Pedro Aquino and Luciano Leonel Mendes

**Abstract**—Orthogonal frequency division multiplexing (OFDM) is a robust and reliable multicarrier modulation scheme that has proven to be adequate for broadband communications. It is widely used in broadcasting and broadband wireless and wireline systems. However, in scenarios where the communication devices are power-limited, such as mobile and satellite communications, OFDM has not been massively used or even not used at all. For instance, OFDM is used only in downlink of 4G networks, while the uplink uses single carrier frequency division multiplexing. One of the main culprits of this is the high peak to average power ratio (PAPR) of the OFDM signal. Reducing the PAPR of the OFDM signals is important for a large variety of application. Several PAPR reduction techniques for OFDM have been proposed recently. The aim of this paper is to present a tutorial about a set of algorithms based on Walsh-Hadamard transform (WHT) for reducing the PAPR of the OFDM symbols. We also propose a new technique, named selective mapping based on WHT without extended information (SLM-WHT-WEI), which does not convey the explicit information to the receiver. We will show that the approaches based on WHT can also improve the OFDM symbol error rate performance over frequency-selective channels. Different schemes based on the properties of the WHT are presented and compared, assuming linear and non-linear channels. The PAPR reduction performance analysis shows that the PAPR can be effectively reduced while good performance in terms of symbol error rate can be achieved even in severely constrained channel conditions.

**Index Terms**—OFDM, PAPR, WHT, SLM, performance analysis.

## I. INTRODUCTION

ORTHOGONAL Frequency Division Multiplexing (OFDM) [1] is used in many telecommunication standards. Wireless transmission systems, like some versions of the Wi-Fi (Wireless Fidelity) [2], employ OFDM because of its robustness against frequency-selective channels. DVB-T (Digital Video Broadcasting-Terrestrial) [3] and ISDB-T (Integrated Service Digital Broadcasting-Terrestrial) [4] also use OFDM for providing high data throughput and flexible configurations for digital television broadcasting. A multiuser version of OFDM, called OFDMA (Orthogonal Frequency Division Multiple Access) has been selected for the Long Term Evolution (LTE) downlink [5] and WiMAX (Worldwide Interoperability for Microwave Access) [6]. IEEE 802.22,

proposed for wireless regional area networks [7], and IEEE 802.11p, developed for vehicle-to-vehicle communications [8], also adopt OFDM in their physical layer (PHY). Lately, OFDM-based waveforms are being considered for the 5th generation of mobile communication (5G) [9].

OFDM became popular due to its low-complexity implementation based on fast Fourier transform algorithms (FFT) and simple equalization performed in the frequency domain [10]. However, OFDM has also disadvantages. Its high peak to average power ratio (PAPR) [11] is an important drawback that hinders its application in power-limited devices. As the number of subcarriers increases, also grows the possibility of having several subcarriers being constructively added, resulting in a signal with high amplitude peaks in the time-domain. If such resulting signals are transmitted through non-linear high power amplifiers (HPA), as the ones used in satellite and mobile phones, the high amplitude peaks will be compressed or even clipped by the amplifier, leading to intermodulation, high out-of-band emission (OOBE) and performance loss due to the intercarrier interference (ICI) [12]. ICI can cause prohibitive degradation of the symbol error rate (SER) performance and increases adjacent channel interference [13]. Incrementing the input power back-off (IBO) reduces the non-linear distortions, but also reduces the amplifier power efficiency, which clearly cannot be applied to energy-limited devices [14].

In order to avoid the problems introduced by the high PAPR presented by OFDM signals, LTE employs single-carrier frequency-domain-equalization (SC-FDE) [15] in the uplink. The low PAPR presented by SC-FDE signals and its good performance under time-variant and frequency-selective makes this waveform suitable for mobile applications. However, although equalization in frequency-domain is an optimal solution for OFDM, it is sub-optimal for single carrier systems [16]. Another disadvantage presented by SC-FDE is the high complexity on the receiver side, which might not be affordable in applications such as Internet of Things [9]. Since most candidates for future generation of mobile networks are OFDM-based, the focus of this paper will be on solutions to reduce the high PAPR of this waveform.

Digital signal processing techniques can be used to reduce the OFDM PAPR and several algorithms have been proposed in the literature [17]. These schemes can be divided into two major groups: i) signal-distortion algorithms and; ii) signal-scrambling algorithms. The algorithms presented in the first group reduce the PAPR by introducing a known and controllable distortion in the OFDM signal before the amplification process. The main signal distortion algorithms are clipping and filtering [18]–[21] and companding [22]–

The Associate Editor coordinating the review of this manuscript and approving it for publication was Prof. Renato Machado.

Guilherme P. Aquino and Luciano L. Mendes was with the Radiocommunication Reference Center (Centro de Referência em Radiocomunicações - CRR) project of the National Institute of Telecommunications (Instituto Nacional de Telecomunicações - Inatel) and CPqD - Brazil. e-mail: guilhermeaquino@inatel.br and luciano1@inatel.br.

Digital Object Identifier: 10.14209/jcis.2017.15.

[24]. Signal-distortion algorithms can significantly reduce the PAPR of the OFDM symbols, but they also introduce in-band and out-of-band interferences that reduce the overall system performance. The signal-scrambling algorithms, on the other hand, reduce the PAPR without distorting the OFDM signal. The main principle consists on mapping the data symbols to a new domain, where the probability of the constructive sum of the subcarriers is reduced. Selective Mapping (SLM) [25]–[28], Partial Transmit Sequence (PTS) [29]–[33] and Walsh-Hadamard Transform (WHT) [11], [34]–[39] are the most well-known algorithms in this category.

With SLM algorithms, several different OFDM symbol are created based on the same transmit data vector. Each of OFDM symbol has a specific PAPR and the one with the lowest PAPR is selected for transmission. The different mappings are generated by multiplying the transmit data vector by a set of  $U$  pseudo-random sequences. The PAPR reduction and the complexity increment depend on the number of different mappings that are generated. For large  $U$ , the probability to transmit a symbol with low PAPR is higher, but it also demands more IFFT blocks on the transmitter side. In addition, the information about the chosen pseudo-sequence used in the transmitter must be sent to the receiver. This explicit information is an overhead that reduces the spectral efficiency and it must be effectively protected against the channel impairments, once an error on this information will result in a complete loss of the OFDM symbol payload.

PTS algorithms employ a different approach for reducing the OFDM PAPR. First, the  $N$  long data vector is segmented into  $V$  different sub-blocks. Then, an  $N$ -point IFFT is applied to each sub-block. After that, the phases of the  $V$  resulting vectors of each sub-block are modified by a set of phase rotation coefficients, where a set of candidate OFDM signals is generated. A selector chooses the OFDM signal with lowest PAPR to be transmitted and also inform the receiver which set of phases has been used to produce the transmitted symbol. As in SLM, an explicit information containing the set of phase coefficients must be protected and transmitted to the receiver. The main difference between SLM and PTS is that the former applies independent phase rotations to each subcarrier, while the latter applies the phase rotations to a group of subcarriers.

Walsh-Hadamard Transform (WHT)-based techniques are the focus of this article. Besides reducing the PAPR, WHT-OFDM can also improve the SER performance of OFDM systems over linear frequency-selective channels [34]. WHT-OFDM presents a weaker PAPR reduction capability when compared with PTS and SLM [40]–[42], but it does not have to convey explicit information to the receiver. Therefore, WHT-OFDM has a higher spectral efficiency and is not exposed to the risk of faulty explicit information. The main drawback of WHT-OFDM is its high sensitivity to clipping distortions, which can lead to prohibitive SER floors under non-linear channels [43], [44]. Three modifications of the WHT-OFDM have been proposed to mitigate this drawback without impacting on the performance gain for linear frequency-selective channels: i) SLM-WHT-OFDM [45]; ii) Double-WHT-OFDM (DWHT-OFDM) [44] and; iii) SLM-DWHT-OFDM [46].

The main objective of this paper is to exploit the principles

and characteristics of these three above-mentioned WHT-based techniques and extend the scheme in [45] in order to remove the need to inform which WHT matrix has been used by the transmitter to the receiver. This extended scheme is named SLM-WHT-WEI (without extended information). The performance, taking into account the PAPR reduction capability and the SER performance over non-linear frequency-selective channels, will be analyzed. The PAPR reduction capability of each technique is measured using the Complementary Cumulative Distribution Function (CCDF) and compared with the conventional OFDM and WHT-OFDM systems. The SER performance of each presented technique is also compared with conventional OFDM and WHT-OFDM systems, taking into account a non-linear frequency-selective channel. An HPA model is considered to simulate the non-linear channel.

In this paper, the notation  $x$ ,  $\mathbf{x}$  and  $\mathbf{X}$  represent a scalar, a vector and a matrix, respectively. The  $n$ th element of a vector  $\mathbf{x}$  is denoted by  $x[n]$ , and  $[\mathbf{X}]_{n,m}$  is the element in  $n$ th row and  $m$ th column of  $\mathbf{X}$ . The notation  $\mathcal{X}$  represents the discrete Fourier transform (DFT) of a vector  $\mathbf{x}$ , while the matrix  $\mathbf{I}_n$  is the identity matrix of size  $n$ .  $\mathbf{0}_{i,j}$  is a zeroed  $i$  by  $j$  matrix. The Hermitian of a matrix is denoted by  $\mathbf{X}^H$ .

This paper is organized as follows: Section II describes the signal model, highlighting the high PAPR of the OFDM signals and its impact on the amplification process. Section III shows the conventional WHT-OFDM principles, exploiting the performance of the technique in terms of PAPR reduction and SER for linear and non-linear frequency-selective channels. Section IV presents SLM-WHT-OFDM and shows its performance gain compared with conventional WHT-OFDM. Double WHT-OFDM (DWHT-OFDM) is presented in Section V, while the principles of SLM-DWHT-OFDM is exploited in Section VI. Section VII brings the final comparisons among all presented schemes. Finally, Section VIII summarizes the conclusions of this paper.

## II. SIGNAL MODEL

Consider a vector  $\mathbf{c}$  with  $N$  complex symbols from an in-phase and quadrature constellation, such as  $M$ -QAM. The OFDM vector  $\mathbf{s}$  carrying the symbol vector  $\mathbf{c}$  is given by

$$\mathbf{s} = \mathbf{F}_N^H \mathbf{c}, \quad (1)$$

where  $\mathbf{F}_N$  is the  $N$  by  $N$  DFT matrix and  $\mathbf{s}$  and  $\mathbf{c}$  are the vectors containing the samples of the sequences  $s[n]$  and  $c[n]$ , respectively.

A cyclic prefix (CP) with  $N_{CP}$  samples are added to the OFDM vector in order to avoid intersymbol interference (ISI) between adjacent OFDM blocks due to channel dispersion [1], leading to

$$\tilde{\mathbf{s}} = \begin{bmatrix} \mathbf{0}_{N_{CP}, N-N_{CP}} & \mathbf{I}_{N_{CP}} \\ & \mathbf{I}_N \end{bmatrix} \mathbf{s}. \quad (2)$$

If the CP is longer than the channel impulse response  $h[n]$ , after removing the CP on the receiver side, the channel can

be modeled using a circulant matrix  $\mathbf{H}$  given by

$$\mathbf{H} = \begin{bmatrix} h_0 & 0 & 0 & \cdots & h_2 & h_1 \\ h_1 & h_0 & 0 & \cdots & h_3 & h_2 \\ \vdots & \vdots & \vdots & \ddots & \vdots & \vdots \\ h_{N_{\text{ch}}-1} & h_{N_{\text{ch}}-2} & h_{N_{\text{ch}}-3} & \cdots & 0 & 0 \\ 0 & h_{N_{\text{ch}}-1} & h_{N_{\text{ch}}-2} & \cdots & 0 & 0 \\ \vdots & \vdots & \vdots & \ddots & \vdots & \vdots \\ 0 & 0 & 0 & \cdots & h_1 & h_0 \end{bmatrix}. \quad (3)$$

After the CP removal, the received vector  $\mathbf{y}$  is given by

$$\mathbf{y} = \mathbf{H}\mathbf{s} + \mathbf{v}, \quad (4)$$

where  $\mathbf{v}$  is the additive white Gaussian noise (AWGN) vector with power spectral density  $N_0$ .

If the channel state information (CSI) is known by the receiver, then the received vector can be easily equalized in the frequency domain by taking a DFT on  $\mathbf{y}$ , as follows:

$$\mathbf{F}_N \mathbf{y} = \mathbf{F}_N \mathbf{H} \mathbf{s} + \mathbf{F}_N \mathbf{v} = \mathbf{F}_N \mathbf{H} \mathbf{F}_N^H \mathbf{c} + \mathbf{F}_N \mathbf{v} = \mathcal{H} \mathbf{c} + \mathcal{V} \quad (5)$$

where  $\mathcal{V}$  is the discrete Fourier transform of  $\mathbf{v}$  and  $\mathcal{H} = \mathbf{F}_N \mathbf{H} \mathbf{F}_N^H$  is a diagonal matrix containing the channel frequency response.

The estimated received symbol is then obtained as:

$$\hat{\mathbf{c}} = \mathcal{H}^{-1} \mathbf{F}_N \mathbf{y} = \mathcal{H}^{-1} \mathcal{H} \mathbf{c} + \mathcal{H}^{-1} \mathcal{V} = \mathbf{c} + \mathcal{H}^{-1} \mathcal{V}. \quad (6)$$

The simplicity and robustness against frequency selective fading are the main reasons that made OFDM very popular in digital communications standards. However, one of the drawbacks of OFDM is the high PAPR of its transmitted signal  $\mathbf{s}$ . In fact, each element of the vector  $\mathbf{s}$  can be modeled as:

$$s[n] = \frac{1}{N} \sum_{k=0}^{N-1} c[k] \exp\left(j2\pi \frac{k}{N} n\right), \quad (7)$$

where  $N$  is the number of subcarriers and  $n = 0, 1, \dots, N-1$  and  $k = 0, 1, \dots, N-1$  are the time and subcarrier indexes, respectively.

Assuming a large number of subcarriers ( $N \geq 16$ ) and that the input symbols  $c[n]$  is a independent and identically distributed discrete sequence with uniform distribution, then, based on the central limit theorem, the amplitude of the OFDM signal can be modeled as a complex Gaussian random variable with variance  $2\sigma_s^2$  [47]. Although the mean value of the OFDM symbol is equal to the data symbol transmitted on the DC subcarrier ( $n = 0$ ), which may, in fact, be chosen to be  $c[0] \equiv 0$ , it is reasonable to model the OFDM symbol as  $s = a + jb$ , where  $a$  and  $b$  are zero-mean Gaussian random variables with variance  $\sigma_s^2$ . Hence,  $s$  is a random variable of the vector  $\mathbf{s}$  defined by (1). It follows that the magnitude envelope of the OFDM symbol, denoted by  $r$ , is a Rayleigh distributed random variable [1] with probability density function given by

$$p_R(r) = \frac{r}{\sigma_s^2} \exp\left(-\frac{r^2}{2\sigma_s^2}\right) \quad r \geq 0, \quad (8)$$

where

$$E[r] = \sigma_s \sqrt{\frac{\pi}{2}} \quad \text{and} \quad \text{VAR}[r] = \sigma_s^2 \left(2 - \frac{\pi}{2}\right). \quad (9)$$

The PAPR of a signal is defined as the ratio between its maximum instantaneous power within a given time frame and its average power during that period. Therefore, the PAPR of an OFDM symbol is given by

$$\text{PAPR}[\mathbf{s}] = \frac{\max[|\mathbf{s}|^2]}{E[|\mathbf{s}|^2]} = \frac{\|\mathbf{s}\|_\infty^2}{2\sigma_s^2}, \quad (10)$$

where  $\|\cdot\|_\infty$  is the  $L - \infty$  norm of a vector.

The complementary cumulative distribution function (CCDF) of the PAPR is an interesting tool to evaluate the behavior of the envelope of an OFDM symbol, once it provides the probability of the PAPR be greater than a given threshold  $x$  [48]. In [49], the authors have proposed an approximation for the CCDF of the PAPR of a continuous-time OFDM signal, stating that

$$P\{\text{PAPR}[s(t)] > x\} = 1 - (1 - e^{-x})^{\alpha N}, \quad (11)$$

where  $s(t)$  is the continuous-time OFDM symbol,  $x$  is a given PAPR threshold and  $\alpha$  is an empirical value, denominated by the oversampling factor, which is equal to 2.8 [49]. Fig. 1 shows the CCDF of the PAPR given by (11) considering  $N = 512, 1024$  and  $2048$ , where it is possible to observe that the PAPR increases with the number of subcarriers. According with (11), the OFDM PAPR does not vary with the modulation order  $M$ . Therefore, the results presented in Fig. 1 describe the values of the PAPR of OFDM signals for any  $M$ -QAM modulation scheme.

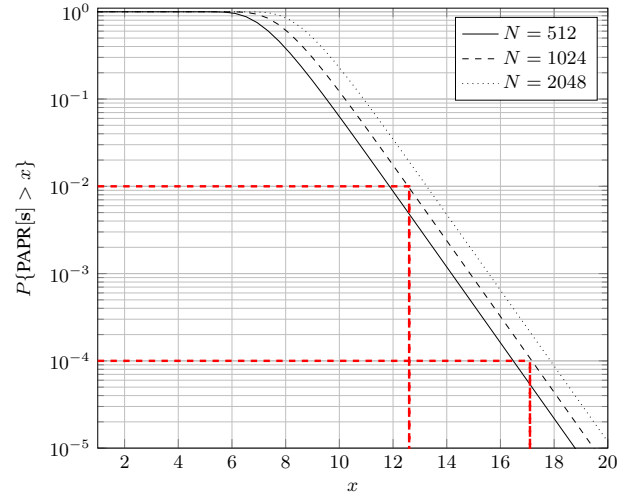


Fig. 1. Complementary cumulative distribution function of the PAPR of the OFDM symbols for  $N = 512, 1024$  and  $2048$   $M$ -QAM modulated subcarriers.

The analysis of the CCDF of the PAPR is fundamental for evaluating the impact of a non-linear amplifier on OFDM signals. Amplifiers are characterized by their power transfer function (PTF) [50]. For an ideal amplifier, the PTF is a straight line, whose slope is the power gain. The PTF of non-linear amplifiers, on the other hand, is divided into a linear and a non-linear region. The boundary between the two regions is at the so-called “1-dB compression point” [51], which is depicted in Fig. 2.

Several models for the input-output relationship of non-linear amplifiers are known. The one used in this paper is based on the solid state power amplifier (SSPA) model [52]. According to this model, the envelope of the signal at the output of the amplifier is given by

$$G[|x(t)|] = \frac{g_0 \cdot |x(t)|}{\left[1 + \left(\frac{g_0 \cdot |x(t)|}{x_{\text{sat}}}\right)^{2p}\right]^{\frac{1}{2p}}}, \quad (12)$$

where  $x(t)$  is the input signal,  $g_0$  is the amplifier gain,  $p$  is the smoothness parameter for the transition between the linear and non-linear regions and  $x_{\text{sat}}$  is the maximum amplitude value that the amplifier can provide at its output. This model was used to obtain the non-linear PTF plotted in Fig. 2.

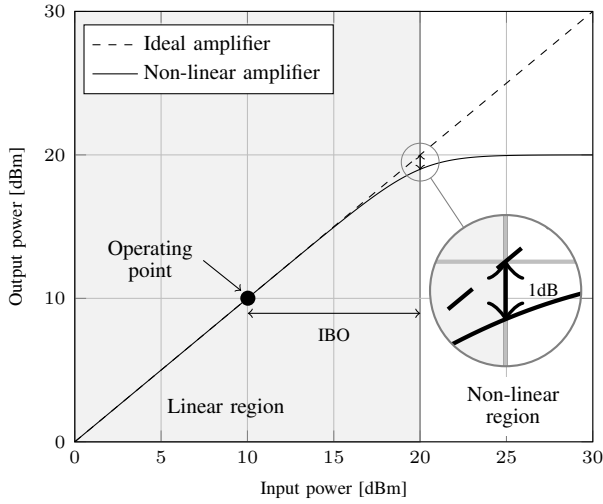


Fig. 2. PTF for ideal and non-linear amplifiers, assuming normalized gain. Parameters for the non-linear amplifier:  $x_{\text{sat}} = 0.3162$ ,  $g_0 = 1$  and  $p = 3$ .

When the smoothness parameter  $p \rightarrow \infty$ , it means that there is an abrupt transition from the linear to the non-linear region, which is a pessimistic situation. This is assumed to be the case in all simulations carried out in this paper in order to obtain the worst case for the nonlinearity in the HPA.

The 1-dB compression point is the best operating point for the amplifier in terms of power efficiency. However, OFDM signals cannot operate at this point because the high peaks of the signal will drive the amplifier to its non-linear region, resulting in a severe clipping of these peaks. In order to prevent this problem, one obvious solution is to introduce an input back-off (IBO) that shifts the operating point well below the 1-dB compression point, as shown in Fig. 2.

The IBO is a power gain defined as

$$P_{\text{IBO}} = 10 \log \left( \frac{x_{\text{sat}}^2}{E[|s(t)|^2]} \right). \quad (13)$$

The amplifier will not clip the transmitted signal when  $P_{\text{IBO}}$  is larger than the OFDM PAPR. The drawback of this approach is the low energy efficiency achieved by the amplifier.

A trade-off between power-efficiency and clipping distortion of the transmitted signal can be achieved using the CCDF of the PAPR, presented in Fig. 1. For example, consider an

OFDM system with  $N = 1024$  subcarriers and an (acceptable) target clipping probability of  $10^{-2}$ . The PAPR curve in Fig. 1 indicates that an IBO of 12.5 in linear scale (or 11 dB in logarithm scale) is necessary in order to avoid the desired level of clipping. If an IBO of 17 in linear scale (or approximately 12 dB) is affordable, then the clipping probability can be reduced to  $10^{-4}$ .

### III. WHT-OFDM

#### A. The Walsh-Hadamard Transform

The WHT is a unitary transform that is used in a range of practical applications [53]. The WHT employed in this paper is based on the Sylvester matrix, also called natural-ordered Hadamard matrix, or Walsh-Hadamard matrix, which can be constructed as follows

$$\mathbf{W}_N = \begin{bmatrix} \mathbf{W}_{N/2} & \mathbf{W}_{N/2} \\ \mathbf{W}_{N/2} & -\mathbf{W}_{N/2} \end{bmatrix}, \quad (14)$$

where  $\mathbf{W}_1 = [1]$ . The matrix in (14) is considered to be a Hadamard matrix since

$$\mathbf{W}_N \mathbf{W}_N^H = \mathbf{W}_N^H \mathbf{W}_N = N \mathbf{I}_N \quad (15)$$

and all elements in  $\mathbf{W}$  belongs to the set  $\{-1, +1\}$ . The Hadamard matrix and its Hermitian are orthogonal to each other, which also means that the columns or rows of the Hadamard matrix are a set of orthogonal vectors. Notice that the Hadamard matrix is symmetric [53].

The Hadamard matrix presented in (14) is used to perform the WHT. In this transform, the elements of the data vector  $\mathbf{c} = [c_0, c_1, \dots, c_{N-1}]^T$  are linearly combined according to the elements of the rows of  $\mathbf{W}$ . Therefore, the WHT of the data is given by

$$c_w[n] = \frac{1}{\sqrt{N}} \sum_{k=0}^{N-1} [\mathbf{W}_N]_{k,n} c[k]. \quad (16)$$

The WHT can also be represented by matrix notation as

$$\mathbf{c}_w = \frac{1}{\sqrt{N}} \mathbf{W}_N \mathbf{c}, \quad (17)$$

while its inverse is given by

$$\mathbf{c} = \frac{1}{\sqrt{N}} \mathbf{W}_N^H \mathbf{c}_w = \frac{1}{\sqrt{N}} \mathbf{W}_N \mathbf{c}_w. \quad (18)$$

#### B. WHT-OFDM

WHT and OFDM can be easily combined in order to reduce the PAPR and improve the robustness against frequency-selective channels [34]. In the WHT-OFDM, the data vector  $\mathbf{c}$ , obtained by mapping the bits vector  $\mathbf{b}$  using a  $M$ -QAM modulator, is applied to the WHT. The resulting coefficients are transmitted using OFDM. On the receive side, after the DFT, the data symbols are recovered applying the WHT on the received coefficients. Fig. 3 shows the block diagram of the WHT-OFDM communication chain.

In this case, the WHT-OFDM transmission vector is given by

$$\mathbf{s}_w = \mathbf{F}_N^H \mathbf{c}_w = \frac{1}{\sqrt{N}} \mathbf{F}_N^H \mathbf{W}_N \mathbf{c}. \quad (19)$$

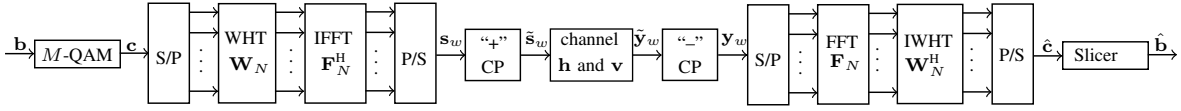


Fig. 3. Block diagram of the WHT-OFDM communication chain.

A CP can be added to the transmitted WHT-OFDM symbol to avoid the ISI under the time dispersive channel, as presented by (1). On the receiver side, the received vector after the CP removal is given by

$$\mathbf{y}_w = \mathbf{H}\mathbf{s}_w + \mathbf{v}. \quad (20)$$

Applying the DFT on the received signal and equalizing in the frequency-domain allows one to recover the transmitted coefficients affected by the channel and corrupted by the AWGN. The recovered data symbols are obtained by applying the inverse WHT to the recovered coefficients, which leads to

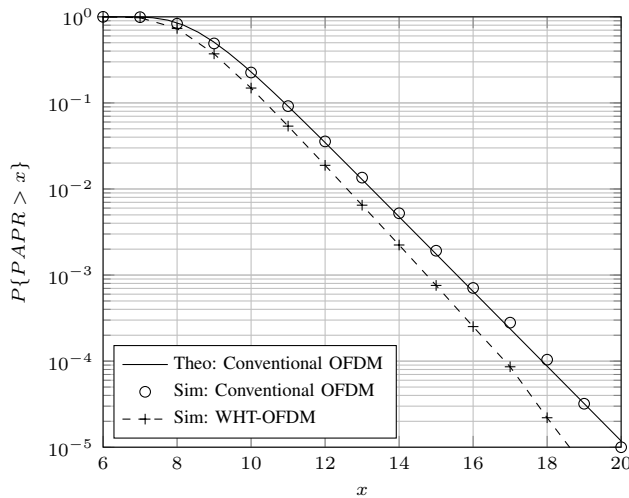
$$\hat{\mathbf{c}} = \frac{1}{\sqrt{N}} \mathbf{W}_N^H \mathcal{H}^{-1} \mathbf{F}_N \mathbf{y}_w = \mathbf{c} + \frac{1}{\sqrt{N}} \mathbf{W}_N \mathcal{H}^{-1} \mathcal{V}. \quad (21)$$

A slicer estimates the received bit vector  $\hat{\mathbf{b}}$  based on  $\hat{\mathbf{c}}$ .

### C. PAPR of the WHT-OFDM signal

The linear combination induced by the Walsh-Hadamard transform reduces the aperiodic correlation of the symbols at the input of the IDFT block [54]. According with [55], a lower correlation between the samples of the vector at the IDFT input ( $\mathbf{c}_w$ ) reduces the maximum PAPR value at the IDFT output ( $\mathbf{s}_w$ ). Therefore, as can be seen in Fig. 4, OFDM presents higher PAPR when compared with WHT-OFDM. Notice that the theoretical curve presented in Fig. 4 is given by (11), which agrees with the computational simulation.

Since WHT-OFDM presents a smaller PAPR, this scheme can be considered more suitable for applications based on power-limited devices.


 Fig. 4. CCDF of PAPR of conventional OFDM and WHT-OFDM symbols.  $N=2048$  and 16-QAM.

### D. WHT-OFDM SER over linear channels

According to (19), each subcarrier employed by the WHT-OFDM carries a linear combination of all data symbols presented in  $\mathbf{c}$ . On the other hand, each subcarrier in OFDM carries a specific data symbol from the vector  $\mathbf{c}$ .

Therefore, if a frequency selective channel introduces a strong attenuation in a given frequency band, the data transmitted in the OFDM subcarriers corresponding to the attenuated band are likely to be received with errors. With WHT-OFDM, a narrow band attenuation introduced by the channel will affect only the coefficient transmitted in the corresponding subcarriers. Since the data symbols are spread over the entire WHT-OFDM bandwidth, the loss of the coefficients in a subset of the subcarriers will slightly affect all data symbols. If the SNR is high enough at the receiver side, then, all data symbols can be reliably recovered, improving the WHT-OFDM SER performance in comparison with OFDM. On the other hand, if the SNR available on the receiver side is low, the spreading of the channel distortion might lead to a degradation in all data symbols from  $\mathbf{c}$ , leading to a poor SER performance.

The above-mentioned effect of the WHT can be seen as a spreading (without bandwidth increase) of the data information  $\mathbf{c}$  in all OFDM bandwidth. Therefore, the WHT introduces frequency diversity to the OFDM system. From (21), it is possible to see that the WHT averages the diagonal matrix channel frequency response, leading to an equivalent channel matrix given by

$$\mathcal{H}_{\text{eq}} = \frac{1}{\sqrt{N}} \mathbf{W}_N \mathcal{H}^{-1}. \quad (22)$$

Once the inverse of a diagonal matrix is obtained by inverting the elements of the main diagonal, the absolute value of the equivalent channel frequency response is given by

$$\mathbf{H}_{\text{eq}} = \left( \sum_{i=0}^{N-1} \frac{1}{N |\mathcal{H}_{i,i}|^2} \right)^{-\frac{1}{2}}. \quad (23)$$

Therefore, the WHT-OFDM SER performance over frequency-selective channels can be directly adapted from the SER performance over AWGN channel, where the SNR is weighted by the equivalent channel gain, leading to

$$p_e \approx \frac{2(L-1)}{L} \text{erfc} \left( \sqrt{\frac{3}{2} \frac{|\mathbf{H}_{\text{eq}}|^2 E_s}{(M-1) N_0}} \right), \quad (24)$$

where  $M$  is the constellation order,  $L = \sqrt{M}$ ,  $E_s$  is the average energy per data symbol,  $N_0$  is the noise spectral power density and  $\text{erfc}(\cdot)$  denotes the Gaussian complementary error function.

Fig. 5 compares (24) with computational simulation results, assuming the following frequency-selective channels: Extended Pedestrian A (EPA), Extended Vehicular A (EVA)

and Extended Typical Urban (ETU) channel models, presented in Table I [56], where  $\tau_n$  and  $\alpha_n$  represent delay and gain of the  $n$ -th channel path, respectively.

TABLE I  
CHANNEL MODELS USED IN THE SIMULATIONS.

EPA		EVA		ETU	
$\tau_n$ [ns]	$\alpha_n$ [dB]	$\tau_n$ [ns]	$\alpha_n$ [dB]	$\tau_n$ [ns]	$\alpha_n$ [dB]
0	0.0	0	0.0	0	-1.0
30	-1.0	30	-1.5	50	-1.0
70	-2.0	150	-1.4	120	-1.0
90	-3.0	310	-3.6	200	0.0
110	-8.0	370	-0.6	230	0.0
190	-17.2	710	-9.1	500	0.0
410	-20.8	1090	-7.0	1600	-3.0
—	—	1730	-12.0	2300	-5.0
—	—	2510	-16.9	5000	-7.0

Table II brings the parameters employed in the simulation results presented in Fig. 5. Perfect channel estimation is assumed.

TABLE II  
SYSTEM PARAMETERS FOR THE SIMULATIONS.

PARAMETER	VALUE
Number of subcarriers ( $N$ )	2048
Modulation order ( $M$ )	16
Cyclic prefix length	512
Sampling rate ( $T_s$ )	10 [ns]

From Fig. 5, it is possible to verify that the gain introduced by the WHT depends on the channel model. The OFDM SER performance variation introduced by the different channel models is more pronounced than the one observed in the WHT-OFDM SER performance. For instance, the performance difference between the three channels observed for WHT-OFDM at a SER of  $10^{-5}$  is 7 dB. For OFDM, for the same SER, there is a variation of 13 dB between EVA and EPA channels. The spreading introduced by the WHT means that the performance depends only on the average gain of the channel impulse response, and not on the variation of the channel response over the frequency, as is the case with OFDM.

*E. SER performance of WHT-OFDM over non-linear channels*

As already shown, the coefficient transmitted by each WHT-OFDM subcarrier is the linear combination of  $N$  data symbols. This procedure reduces the PAPR, however, when a clipping occurs in a component of the WHT-OFDM signal, the error caused by this clipping is distributed to all data symbols, increasing the distance between the expected and received symbol. In order to verify this statement, let  $\epsilon$  be the Euclidean distance between the received and expected symbol, i.e.,  $\epsilon = \|\hat{c}_n - c_n\|^2$ . Fig. 6 presents the probability of  $\epsilon$  be larger than a determined value  $\epsilon_0$ ,  $P(\epsilon > \epsilon_0)$ . Notice that, in Fig. 6, a comparison is made in terms of the CCDF of the difference between the transmitted and received 16-QAM symbols, assuming OFDM and WHT-OFDM over a non-linear channel as characterized by Fig. 2.

Fig. 6 shows that errors below  $\epsilon < 0.5$  have a higher probability of occurrence in conventional OFDM. However,

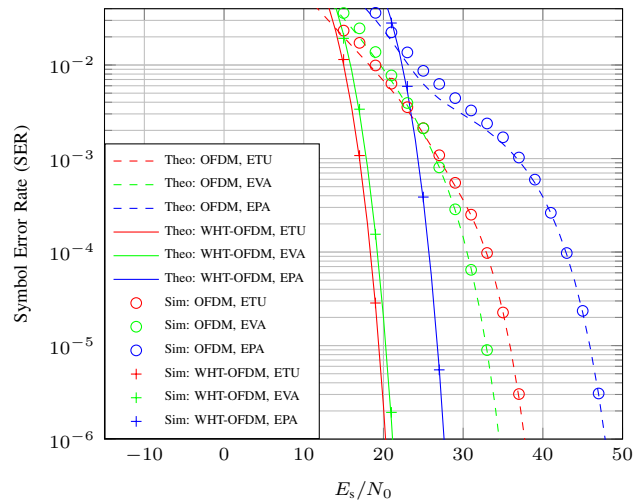


Fig. 5. Symbol error rate of OFDM and WHT-OFDM under frequency selective channel.

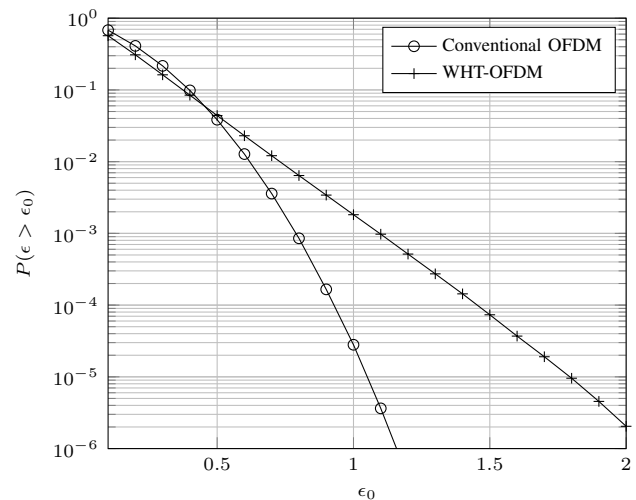


Fig. 6. CCDF of the error caused by clipping in OFDM and WHT-OFDM systems.

this error does not lead to a wrong decision by the slicer, since the minimum Hamming distance is 2. WHT-OFDM has a higher probability of presenting errors above  $\epsilon = 0.5$ , which means that the non-linearities introduced by the channel are more harmful to WHT-OFDM than to OFDM. Therefore, the WHT-OFDM SER over non-linear channels presents a high error floor, as can be observed in Fig. 7, where it is also possible to notice that WHT-OFDM has a better performance than OFDM only for small SNR more precisely for  $15\text{dB} < E_s/N_0 < 25\text{dB}$ . In this SNR range, the effect of the channel selectivity is more pronounced than the effect of the clipping. Therefore, the diversity introduced by WHT-OFDM leads to a performance gain over OFDM. On the other hand, the WHT-OFDM presents low SER performance than conventional OFDM system when the clipping effect is more evident than the fading effect. It occurs for  $E_s/N_0 > 25$  dB under the ITU-EVA channel.

The error floor introduced by the clipping in WHT-OFDM

cannot be compensated by the diversity gain obtained by spreading the information over several subcarriers. Therefore, the WHT-OFDM is not recommended for non-linear frequency-selective channels.

#### F. ZF versus MMSE Equalizer

As can be seen in (6) and (21), the received OFDM and WHT-OFDM symbols,  $\hat{c}$ , are obtained using a zero-forcing (ZF) equalizer [57]. However, it is worth mentioning that these data symbols can be estimated using a minimum mean square error (MMSE) equalizer [57]. In this case, the estimation of the data symbols is given by

$$\hat{c} = \mathbf{H}_{\text{MMSE}} \mathbf{y}, \quad (25)$$

where  $\mathbf{y}$  is the received vector and  $\mathbf{H}_{\text{MMSE}}$  is MMSE equalization matrix, defined as

$$\mathbf{H}_{\text{MMSE}} = \left( \mathbf{A}^H \mathbf{A} + \frac{1}{\gamma} \mathbf{I}_N \right)^{-1} \mathbf{A}^H, \quad (26)$$

where  $\mathbf{A}$  is effective channel matrix, defined as  $\mathbf{A} = \mathbf{H} \mathbf{F}_N^H$  for OFDM and  $\mathbf{A} = \mathbf{H} \mathbf{F}_N^H \mathbf{W}_N$  for WHT-OFDM.

Fig. 7 shows the OFDM and WHT-OFDM SER performance in a non-linear frequency-selective channel using ZF and MMSE. MMSE equalizer brings a small improvement for WHT-OFDM in low SNR, where the frequency-selectiveness of the channel is more relevant. For the OFDM scheme, the SER performance remains the same, as expected. The error-floor in both schemes does not change, because the nonlinearity caused by the clipping cannot be solved with neither the ZF or MMSE equalizers. Therefore, the choice of the equalizer does not change the main conclusions about the SER performance of the analyzed schemes, so, the others SER performance results are obtained assuming that ZF equalizer is employed.

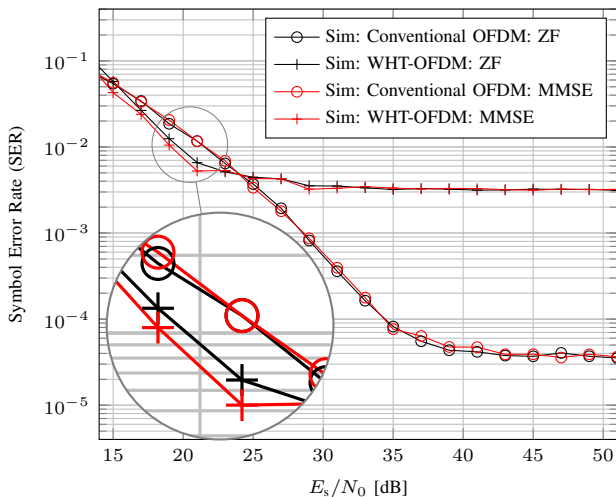


Fig. 7. OFDM and WHT-OFDM SER assuming ZF and MMSE equalizers under linear and non-linear ITU-EVA channels.

#### IV. SLM-WHT-OFDM

Although WHT-OFDM is not a good choice for non-linear frequency-selective channels, it is possible to increase its SER performance under these conditions, while maintaining the diversity gain. One approach that can be used to improve the WHT-OFDM SER performance consists of applying the selective mapping (SLM) combined with the WHT, leading to SLM-WHT-OFDM [45]. Fig. 8 depicts the communication chain of this scheme.

Next subsections detail this technique.

##### A. SLM-WHT-OFDM

As mentioned in Section I, the SLM technique creates a set of  $U$  signals that convey the same information, but, with different characteristics. SLM-WHT-OFDM employs different Walsh-Hadamard matrices to produce  $U$  different versions of the WHT-OFDM symbol. These matrices can be obtained by permuting columns of the original Walsh-Hadamard matrix. Some examples are shown in (27), where  $\mathbf{W}_{41}$  is the original Walsh-Hadamard matrix and  $\mathbf{W}_{42}$  is obtained by permuting the first and second columns of  $\mathbf{W}_{41}$ .

$$\mathbf{W}_{41} = \begin{bmatrix} +1 & +1 & +1 & +1 \\ +1 & -1 & +1 & -1 \\ +1 & +1 & -1 & -1 \\ +1 & -1 & -1 & +1 \end{bmatrix}, \quad (27)$$

$$\mathbf{W}_{42} = \begin{bmatrix} +1 & +1 & +1 & +1 \\ -1 & +1 & -1 & +1 \\ +1 & +1 & -1 & -1 \\ -1 & +1 & +1 & -1 \end{bmatrix}.$$

It is important to observe that the permutations of the columns of  $\mathbf{W}_N$  still preserve the orthogonality properties between rows and columns of the new matrices [58], since these matrices are also Hadamard matrices because (15) is still respected.

Therefore, as in SLM schemes, the SLM-WHT-OFDM technique uses  $U < N$  different matrices to create  $U$  versions of the WHT-OFDM symbol, each one with different statistics. A selector chooses the signal with lower PAPR among the set of  $U$  generated signals, as depicted in Fig. 8. Therefore, the SLM-WHT-OFDM transmission signal can be expressed by

$$\mathbf{s}_{w \min} = \arg \min_{u \in \{1, 2, \dots, U\}} \left\{ \text{PAPR} \left[ \frac{1}{\sqrt{N}} \mathbf{F}_N^H \mathbf{W}_{Nu} \mathbf{c} \right] \right\}, \quad (28)$$

where  $\mathbf{W}_{Nu}$  is the  $u$ th version of the Walsh-Hadamard matrix. Here, a CP is also used to protect  $\mathbf{s}_{w \min}$ , resulting in  $\tilde{\mathbf{s}}_{w \min}$ . The matrix used to generate the symbol with lower PAPR must be known by the receiver. Therefore, a robust link must be used to carry the index  $I_{\min}$  that indicates which matrix has been used on the transmission side.

Let's  $\tilde{\mathbf{y}}_w$  be a noisy and corrupted version of  $\tilde{\mathbf{s}}_{w \min}$  on the receiver side. The estimated data symbols are obtained after removing the CP, applying the FFT and the inverse WHT using the proper Walsh-Hadamard matrix identified by  $I_{\min}$ , as depicted by Fig. 8.

Clearly, the complexity increment of the SLM-WHT-OFDM is restricted to the transmitter side, since the receiver side

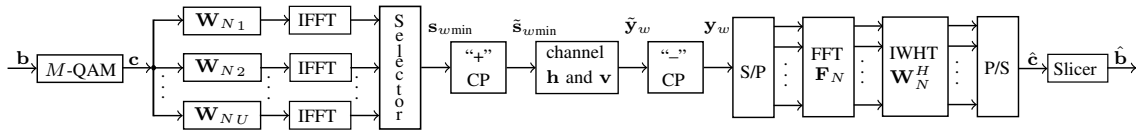


Fig. 8. Block diagram of the SLM-WHT-OFDM communication chain.

implements the same procedures employed by the WHT-OFDM scheme.

**B. PAPR of the SLM-WHT-OFDM signal**

SLM-WHT-OFDM has a small PAPR compared with conventional OFDM and WHT-OFDM, as can be seen in Fig. 9, assuming the values presented in Table II.

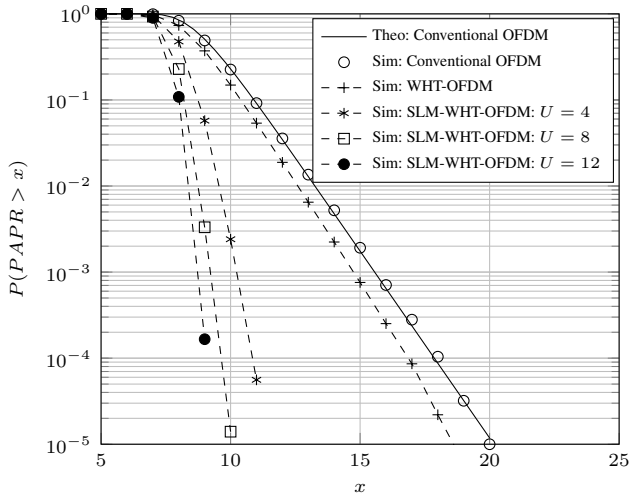


Fig. 9. CCDF of the PAPR assuming OFDM, WHT-OFDM and SLM-WHT-OFDM for  $U = \{4, 8 \text{ and } 12\}$ .

Again, high values of  $U$  increases the probability of finding a SLM-WHT-OFDM symbol with low PAPR, but it also increases the transmitter complexity and the amount of explicit information to be transmitted as overhead.

On the receiver side, only one FFT and a single WHT must be computed for each SLM-WHT-OFDM symbol. Therefore, the increment in the receiver complexity is negligible when compared with conventional WHT-OFDM receivers.

**C. SLM-WHT-OFDM SER performance under linear channels**

SLM-WHT-OFDM achieves the same diversity gain observed for WHT-OFDM over frequency-selective channels, as can be seen in Fig. 10.

As shown in Fig. 10, SLM-WHT-OFDM SER performance over linear channels is not affected by  $U$  and, therefore, (24) can be used to estimate the SER performance of this scheme. It means that SLM-WHT-OFDM also spreads the information over all subcarriers, allowing the receiver to harvest diversity gain over frequency-selective channels.

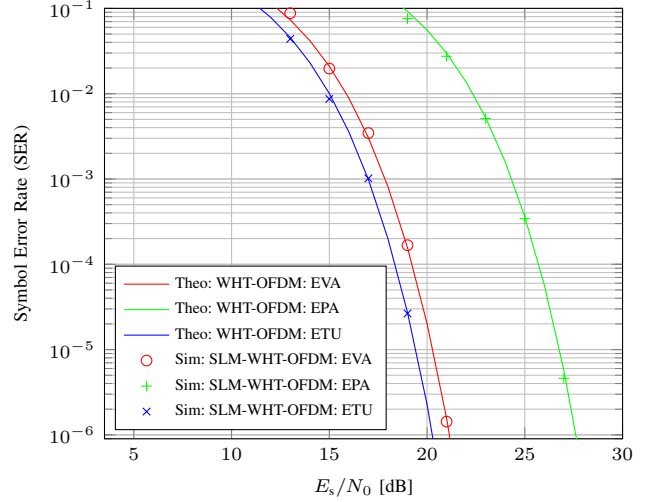


Fig. 10. SLM-WHT-OFDM SER performance under linear frequency-selective channels.

**D. SER performance of the SLM-WHT-OFDM under non-linear channels**

Since SLM-WHT-OFDM has considerably smaller PAPR compared with WHT-OFDM, the probability of having a clipped signal is also significantly reduced. Therefore, SLM-WHT-OFDM outperforms OFDM and WHT-OFDM over non-linear frequency selective channels, as can be seen in Fig. 11 for different values of  $U$  and the parameters presented in Table. II.

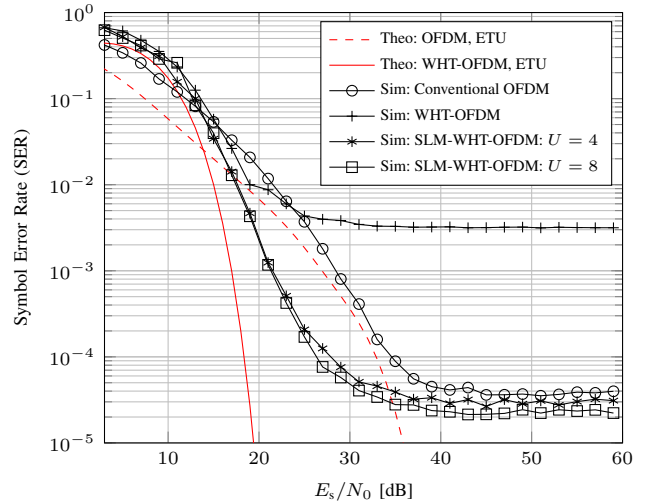


Fig. 11. OFDM, WHT-OFDM and SLM-WHT-OFDM SER under non-linear ETU channel.

Fig. 11 shows that the SLM-WHT-OFDM error floor is

lower than the other schemes, as expected. Also, SLM-WHT-OFDM SER performance improves as  $U$  increases, although the performance gain obtained in Fig. 11 is marginal when varying  $U$  from 4 to 8. This means that  $U$  can be chosen as a trade-off between complexity increment on the transmitter side and SER performance under non-linear channels.

### E. SLM-WHT-OFDM without explicit information

The transmission of the explicit information is a drawback of the SLM-OFDM schemes, since it reduces the spectrum efficiency and might lead to a loss of an entire SLM-OFDM symbol when this information is received erroneously on the receiver side. In order to avoid these problems, we propose a new scheme named SLM-WHT-OFDM Without Explicit Information (WEI). In this scheme, the index  $I_{\min}$  is not transmitted to the receiver. A correlation between the received signal and all possible WHT matrices is used as metric to discover the matrix employed by the transmitter. The matrix that leads to the higher correlation index is used to retrieve the data symbols. This procedure increases the receiver complexity, since  $U$  Walsh-Hadamard transform need to be performed in order to identify the matrix  $\mathbf{W}_{N_u}$  used by the transmitter. Therefore, while the SLM-WHT-OFDM receiver performs only one WHT, the SLM-WHT-WEI receiver performs  $U + 1$  WHTs, where  $U$  WHTs are performed for identifying the correct matrix used by the transmitter and one WHT is performed to recover the data symbols. Fig. 12 shows the block diagram of the procedure used to identify the correct matrix employed by the transmitter.

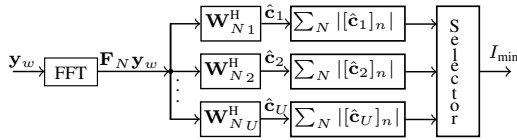


Fig. 12. Block diagram employed on the receiver side to identify the Walsh-Hadamard matrix used by the transmitter.

Hence, the estimated index of the matrix employed on the transmitter side is given by

$$I_{\min} = \arg \max_{u \in \{1, 2, \dots, U\}} \left\{ \sum_{n=0}^{N-1} |[\mathbf{W}_{N_u}^H \mathbf{F}_N \mathbf{y}_w]_n| \right\}. \quad (29)$$

Fig. 13 shows the SLM-WHT-WEI SER performance under non-linear frequency-selective ETU channel. Notice that the SLM-WHT-WEI performs as SLM-WHT-OFDM. Therefore, SLM-WHT-WEI keeps the same performance in terms of SER under non-linear channels as SLM-WHT-OFDM, but it eliminates the need for transmission of the side information, increasing the overall system spectrum efficiency. Also, this modification does not affect the PAPR performance. Therefore, the PAPR CCDF for the SLM-WHT-OFDM-WEI scheme equals the PAPR CCDF obtained for the SLM-WHT-OFDM.

## V. DWHT-OFDM

As shown in Section IV, the SLM-WHT-OFDM scheme has lower PAPR and equivalent SER performance under non-linear

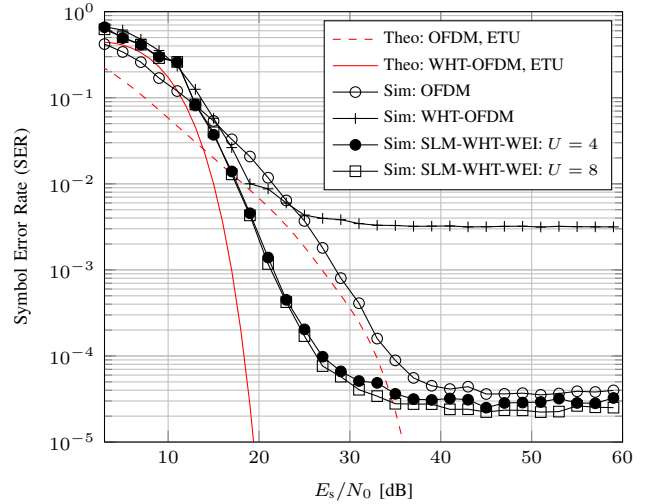


Fig. 13. SER for conventional OFDM, WHT-OFDM and SLM-WHT-WEI with different values of  $U$  under non-linear ETU channel.

channels when compared with OFDM. The cost of using such technique is the complexity increment of the transmitter and, in the case of SLM-WHT-OFDM-WEI, also of the receiver. A solution to overcome this issue, based on applying different WHT on the real and imaginary parts of the QAM data symbols, was presented in [44]. This proposed scheme does not aim for PAPR reduction, and only improves the SER performance under non-linear channels, eliminating the high SER error-floor. Fig. 14 depicts the block diagram of the Double WHT-OFDM (DWHT-OFDM) communication chain, while next subsections bring more details about this approach.

### A. The Double WHT-OFDM system

Clipping the WHT-OFDM signal leads to the SER error floor under non-linear channels. The DWHT-OFDM scheme increases the robustness against clipping since the real and imaginary parts of the data symbol are spread through the subcarriers using different matrices obtained by permuting the columns of the Walsh-Hadamard matrix [44], as presented in (27).

Let  $\mathbf{W}_{N_1}$  and  $\mathbf{W}_{N_2}$  be two Walsh-Hadamard matrices with different columns permutations. The DWHT can be defined as

$$\mathbf{c}_w = \frac{1}{\sqrt{N}} \{ (\mathbf{W}_{N_1}) \Re(\mathbf{c}) + j (\mathbf{W}_{N_2}) \Im(\mathbf{c}) \}, \quad (30)$$

while the Inverse DWHT is given by

$$\hat{\mathbf{c}} = \frac{1}{\sqrt{N}} \{ (\mathbf{W}_{N_1}^H) \Re(\mathbf{c}_w) + j (\mathbf{W}_{N_2}^H) \Im(\mathbf{c}_w) \}. \quad (31)$$

As in the conventional WHT-OFDM, the coefficients obtained by (30) are applied to an OFDM scheme for transmission under the non-linear multi-path channel, as shown in Fig. 14.

It is worth mentioning that the DWHT-OFDM and WHT-OFDM computational complexities are equivalent. In practice, WHT consists on two matrices product between real and

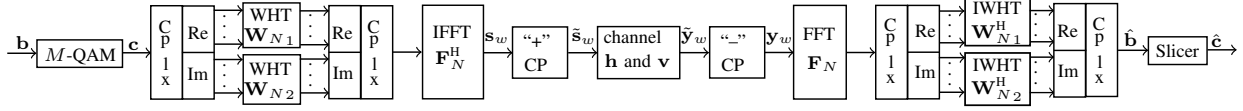


Fig. 14. Block diagram of DWHT-OFDM communication chain.

imaginary parts of the data vector and the conventional Walsh-Hadamard matrix. In the DWHT-OFDM, the same procedure is required, however, using different matrices for the real and imaginary parts of the data vector.

**B. DWHT-OFDM PAPR analysis**

The DWHT-OFDM PAPR performance equals the one observed for conventional OFDM, as can be seen in Fig. 15.

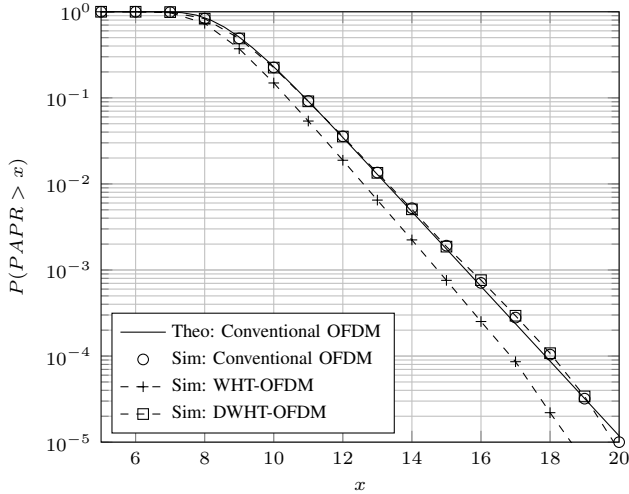


Fig. 15. PAPR CCDF for conventional OFDM, WHT-OFDM and DWHT-OFDM.

Clearly, this schemes does not bring any advantage in terms of PAPR when compared with OFDM.

**C. DWHT-OFDM SER performance under linear channels**

Once again, (24) can be used to estimate the DWHT-OFDM SER performance over linear channels, which means that DWHT-OFDM achieves the same diversity gain observed in conventional WHT-OFDM, as can be seen in Fig. 16.

**D. DWHT-OFDM SER performance under non-linear channels**

As mentioned previously, this scheme aims for improving the robustness of the WHT-OFDM signal against the clipping introduced by the non-linear channel, while keeping the diversity gain collected under linear channels, by decreasing the modulation error caused by the signal clipping.

Fig. 17 compares the modulation error CCDF introduced by clipping in OFDM, WHT-OFDM and DWHT-OFDM symbols.

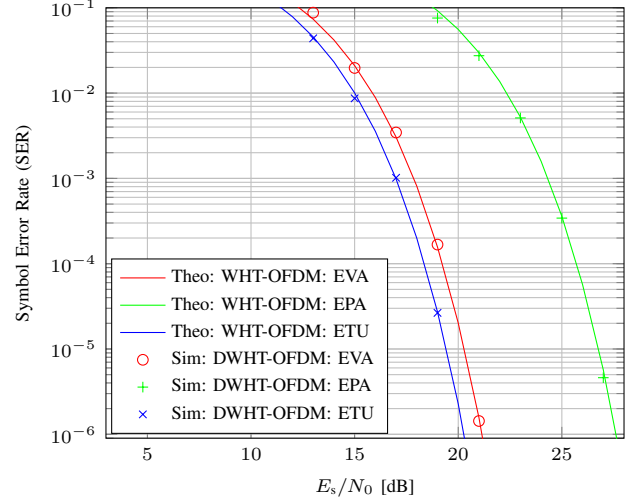


Fig. 16. SER performance of DWHT-OFDM in linear frequency-selective channels

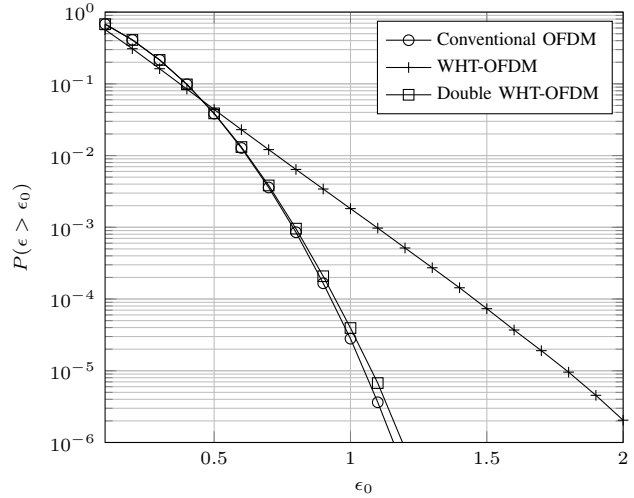


Fig. 17. Modulation error CCDF for OFDM, WHT-OFDM and DWHT-OFDM schemes assuming a non-linear channel.

As can be seen, OFDM and DWHT-OFDM achieve the same modulation error CCDF, while WHT-OFDM under performs the other two schemes.

Fig. 18 compares the SER performance of OFDM, WHT-OFDM and DWHT-OFDM under a non-linear ETU channel. As expected, the DWHT-OFDM outperforms WHT-OFDM, showing that the use of two different matrices performing independent independent WHTs in the real and imaginary components culminates in a more robust system against non-linearities. Also, the DWHT-OFDM outperforms the conventional OFDM system in the region where  $12 < E_s/N_0 < 35$  dB. For

this particular SNR range, the channel frequency-selectivity is more harmful than clipping for the SER performance.

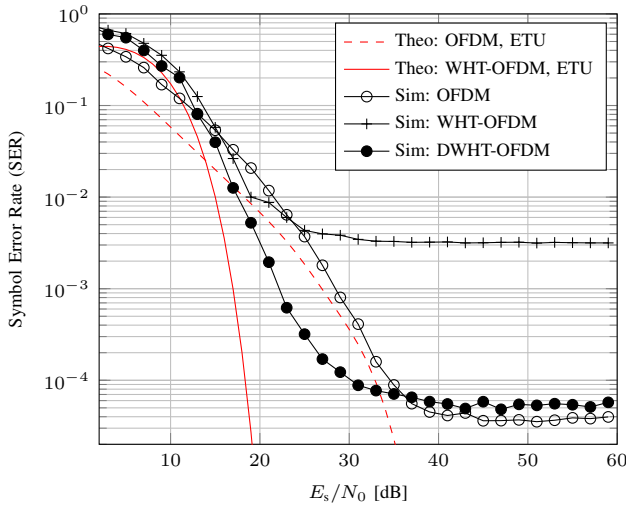


Fig. 18. SER performance for OFDM, WHT-OFDM and DWHT-OFDM under non-linear ETU channel.

Therefore, DWHT-OFDM can provide robustness for the WHT-based OFDM system against the non-linearities, while maintaining the diversity gain harvested in linear channels.

## VI. SLM-DWHT-OFDM

As already seen in Section V, DWHT is an interesting solution for improving SER performance under linear and non-linear frequency-selective channels. However, DWHT-OFDM has high PAPR, like OFDM. On the other hand, SLM allows for a significant PAPR reduction, but without increasing the SER performance in frequency-selective channels. By combining these two approaches, it is possible to achieve low PAPR and harvest the frequency diversity gain simultaneously. The SLM-DWHT-OFDM [46] achieves this goal, as will be presented in the following.

### A. SLM-DWHT-OFDM principles

Fig. 19 depicts the SLM-DWHT-OFDM transmitter. As in DWHT-OFDM, this scheme uses a set of different Walsh-Hadamard matrices obtained by permuting the columns of  $\mathbf{W}_N$ . However, in this case, a set of  $U$  matrices  $[\mathbf{W}_{N_1}; \mathbf{W}_{N_2}; \dots; \mathbf{W}_{N_U}]$  are previously defined and two matrices  $\mathbf{W}_{N_f}$  and  $\mathbf{W}_{N_g}$  are chosen to spread the real and imaginary parts of the data symbol. The vector  $\mathbf{c}_{w_u}$  originated of this DWHT is applied in the block that computes the IFFT, generating the signal in time-domain  $\mathbf{s}_w$ . A selector calculates the PAPR of  $\mathbf{s}_w$  and compares it with the maximum allowed PAPR ( $PAPR_{\max}$ ). If the  $\mathbf{s}_w$  PAPR is lower than  $PAPR_{\max}$ , this signal is transmitted with the indexes corresponding to the both matrices ( $I_w$ ). If the  $\mathbf{s}_w$  PAPR is higher than  $PAPR_{\max}$  a new pair of Walsh-Hadamard matrices is selected to generate a new vector  $\mathbf{c}_{w_u}$ . This process is repeated until a PAPR smaller than  $PAPR_{\max}$  is obtained or all  $U^2$  possible combination of matrices is reached. In this last case, the signal with smallest PAPR is transmitted.

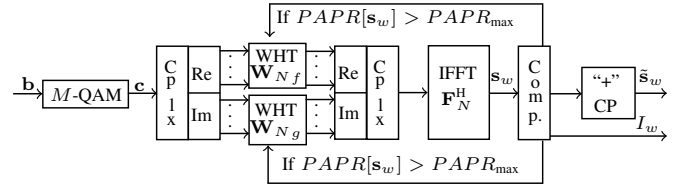


Fig. 19. Block diagram of the SLM-DWHT-OFDM transmitter.

On the receiver side, the indexes  $I_w$  are used to select the two matrices in order to perform the IDWHT. From this point on, the SLM-DWHT-OFDM receiver operates exactly as the DWHT-OFDM receiver. The number of bits used to transmit the explicit information in the SLM-DWHT-OFDM scheme is given by

$$N_c = \lceil \log_2(U^2) \rceil. \quad (32)$$

### B. SLM-DWHT-OFDM PAPR analysis

The PAPR CCDF of the SLM-DWHT-OFDM symbols is shown in Fig. 20, assuming the parameters described in Table II.

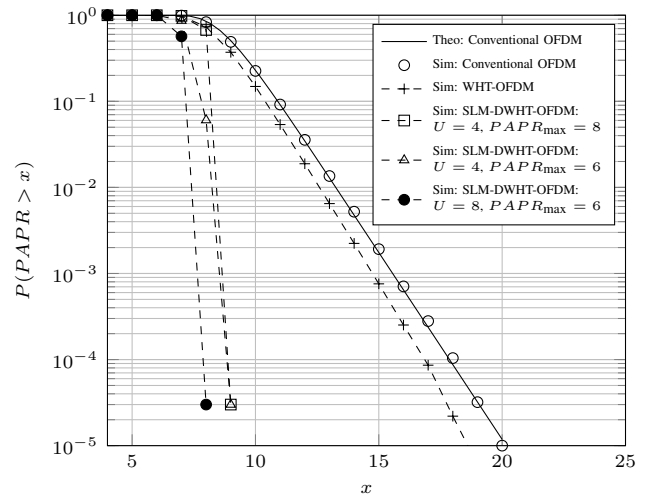


Fig. 20. CCDF PAPR for OFDM, WHT-OFDM and SLM-DWHT-OFDM with different values of  $U$  and  $PAPR_{\max}$ .

From Fig. 20, it is possible to notice that SLM-DWHT-OFDM is able to considerably reduce the PAPR of the transmitted signal. The achieved PAPR depends on the number of available matrices  $U$  and the maximum tolerable PAPR ( $PAPR_{\max}$ ).

Typically, the number of interactions necessary to achieve  $PAPR_{\max}$  increases as the maximum tolerable PAPR reduces, as can be seen in Fig. 21, where the probability mass function of the number of necessary iterations to transmit a given SLM-DWHT-OFDM symbol with acceptable PAPR is shown.

Fig. 21 shows that, for this example, approximately 50% of the SLM-DWHT-OFDM symbols are transmitted in the first iteration when a high  $PAPR_{\max}$  is acceptable and, when the requested PAPR is low, all possible combinations are tried out and the symbol with lowest PAPR (typically larger than the specified one) is transmitted in almost 95% of the cases.

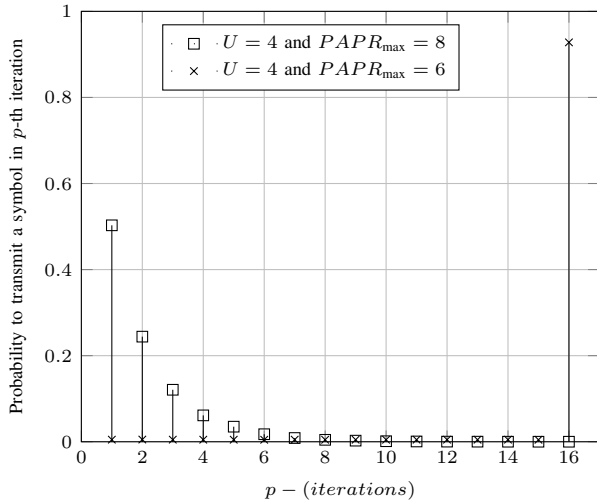


Fig. 21. Number of necessary iterations until transmitting a SLM-DWHT-OFDM symbol.

Table III shows the average number of interactions necessary to achieve a given PAPR with  $U = 4$  and  $U = 8$ .

TABLE III

AVERAGE OF NUMBER OF ITERATIONS TO ACHIEVE THE DESIRED PAPR FOR A SLM-DWHT-OFDM SYMBOL.

	PAPR			
	5	6	7	8
$U = 4$	16.00	15.42	6.28	2.02
$U = 8$	64.00	54.91	1.77	2.04

Clearly, the complexity of the SLM-DWHT-OFDM transmitter depends on the choice of parameters  $U$  and  $PAPR_{max}$ . According to the results shown in the Table III, one can notice that for  $U = 4$  and  $PAPR_{max} = 7$ , in average, 6.28 iterations are necessary to obtain an SLM-DWHT-OFDM symbol. In other words, is necessary to calculate 6.28 DWHTs and IFFTs until the SLM-DWHT-OFDM symbol is transmitted. Therefore, the complexity of the transmitter SLM-DWHT-OFDM is will depend on the average number of iterations, while the receiver complexity equals the complexity to the DWHT-OFDM receiver.

C. SLM-DWHT-OFDM SER performance under linear channels

The SLM-DWHT-OFDM performs as the DWHT-OFDM or SLM-WHT-OFDM under linear channels. Therefore, (24) can be used to estimate the SER performance of this scheme. Since a plot for the SLM-DWHT-OFDM SER performance will be equal to Figs. 10 and 16, the performance curves for this scheme will be omitted.

D. SER performance of SLM-DWHT-OFDM over non-linear channels

Fig. 22 shows the SLM-DWHT-OFDM SER performance under a non-linear frequency-selective channel and compares

it with SER performance of conventional OFDM and WHT-OFDM, assuming the parameters shown in Table II. It is also assumed that  $PAPR_{max} = 8$ . One can observe from Fig. 22 that SLM-DWHT-OFDM improves the system performance under non-linear channels. The number of different Walsh-Hadamard matrices  $U$  does not significantly affect the overall SER performance.

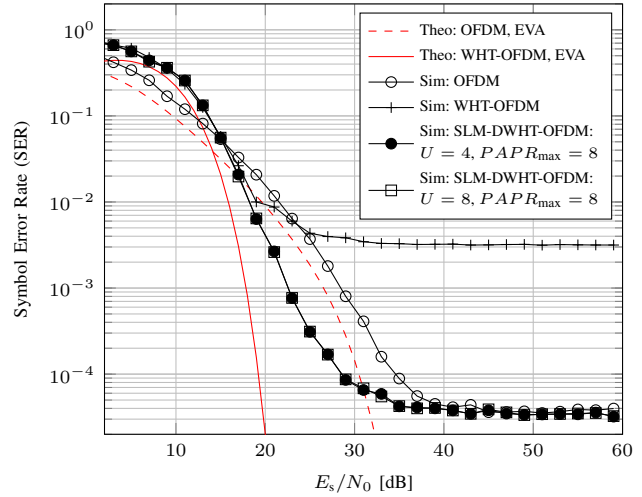


Fig. 22. Symbol error rate of conventional OFDM, WHT-OFDM and SLM-DWHT-OFDM over non-linear EVA channel.

Fig. 23 compares the SLM-DWHT-OFDM SER performance with the performance obtained by OFDM and WHT-OFDM assuming  $PAPR_{max} = 6$ . Clearly, when  $PAPR_{max}$  is more restrictive, the SLM-DWHT-OFDM error-floor decreases. Furthermore, higher values of  $U$  will increase the probability of finding a symbol with lower PAPR below the requested value, at the cost of higher transmission latency and a lower spectral efficiency due to the explicit information.

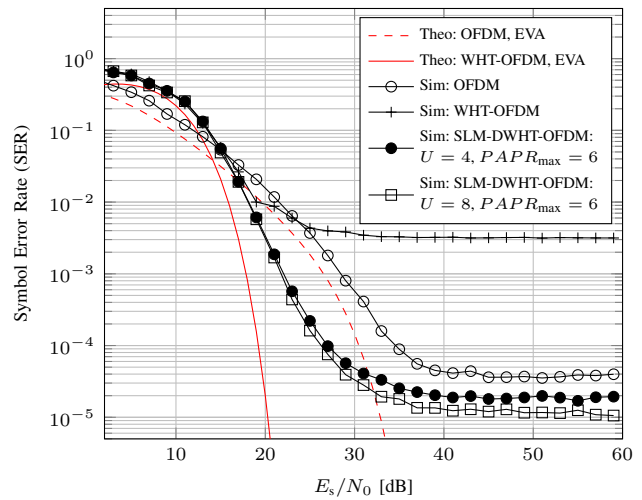


Fig. 23. Symbol error rate of conventional OFDM, WHT-OFDM and SLM-DWHT-OFDM over non-linear EVA channel.

VII. FINAL COMPARISONS

In this section, all schemes described in this paper are compared. Firstly, Fig. 24 brings a comparison in terms of the CCDF of the PAPR of the discussed schemes. It is possible to notice that conventional OFDM and DWHT-OFDM has presented the highest PAPR values, while WHT-OFDM scheme presents approximately 2 dB improvement over OFDM. SLM-WHT-OFDM with  $U = 8$  matrices has presented a significant PAPR reduction when compared with OFDM. The best PAPR reduction has been achieved by SLM-DWHT-OFDM scheme with  $U = 8$  and  $PAPR_{max} = 6$ . Table IV qualitatively summarizes this comparison.

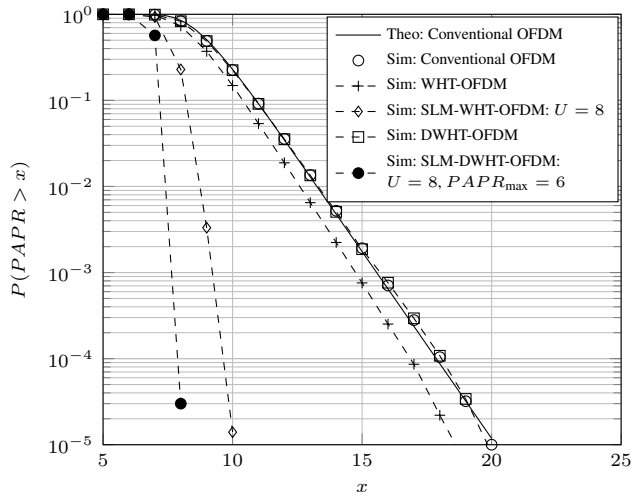


Fig. 24. Comparison of the PAPR CCDF of OFDM, WHT-OFDM, SLM-WHT-OFDM and SLM-DWHT-OFDM.

Fig. 25 compares the SER performance of the schemes described in this paper under non-linear channel. WHT-OFDM has presented the highest error floor. DWHT-OFDM improves the SER performance compared with WHT-OFDM, but it still presents an error floor above conventional OFDM. SLM-WHT-OFDM and SLM-WHT-OFDM-WEI with  $U = 8$  outperforms OFDM and the best SER performance among all analyzed schemes is achieved by SLM-DWHT-OFDM with  $U = 8$  and  $PAPR_{max} = 6$ . Again, Table IV qualitatively compares the SER performance of the considered schemes, assuming a non-linear channel. This table also compares the transmitter and receiver complexities and it lists the schemes that requires the explicit information on the receive side.

### VIII. CONCLUSIONS

OFDM is largely employed in several wireless standards due its high spectrum efficiency and simple implementation based on fast Fourier transform algorithms. However, OFDM symbols present high PAPR, which limits the use of this technique in power limited applications. Moreover, clipping introduced by the non-linear power amplifier leads to spectrum regrowth and high SER.

Using WHT jointly with OFDM presents two major advantages: i) the reduction in the PAPR symbols and ii) a better SER performance under linear frequency-selective channels. However, the SER performance of the WHT-OFDM under

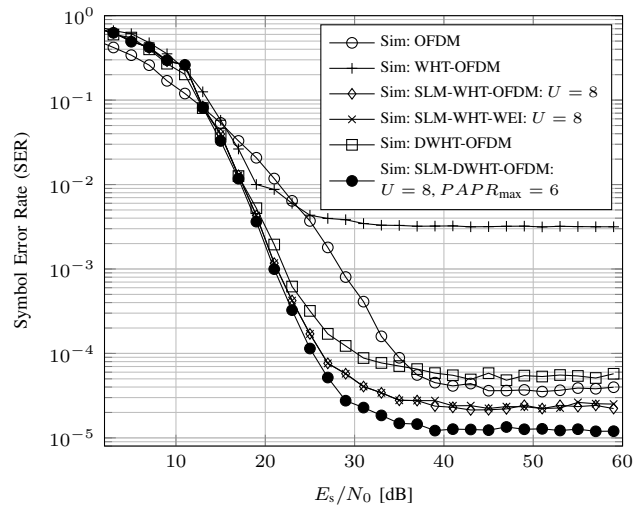


Fig. 25. Comparison of the OFDM, WHT-OFDM, SLM-WHT-OFDM and SLM-DWHT-OFDM SER performance under non-linear ETU channel.

non-linear channels is poor. This performance can be improved by employing the DWHT-OFDM but, in this case, without reducing the PAPR. The DWHT brings the benefits of the Walsh-Hadamard transform for the OFDM systems, even when the channel is non-linear with a small increase in the complexity.

On the other hand, SLM-WHT-OFDM can be used to reduce the PAPR while keeping the performance gain introduced by WHT. With the WEI modification introduced to SLM-WHT-OFDM, which is an original contribution of this paper, no explicit information needs to be sent to the receiver, improving the system spectrum efficiency at the cost of higher complexity on the receiver side.

Finally, the SLM-DWHT-OFDM presents complementary benefits of the SLM and DWHT for OFDM systems operating in non-linear frequency-selective channels. The SLM technique reduces the PAPR, while the DWHT increase the performance in frequency-selective channels and, moreover, decreases the sensibility of the signals against the clipping. The main drawback of this technique is the higher transmitter complexity.

Therefore, OFDM systems employing WHT-based algorithms to reduce the PAPR and increase the SER performance under non-linear and frequency selective channels is an interesting solution for employing multicarrier waveform in application where the transmit signal is likely to lead the amplifier to the non-linear operation.

As a future work, it is interesting to compare these proposed WHT-based schemes with other pre-coding OFDM techniques. Other uniform transforms based on Fourier Matrix, constant amplitude zero auto-correlation (CAZAC) matrix, discrete Hartley matrix, among others, that can be used as pre-coding instead of WHT matrix used in this paper. Interesting SER performance and PAPR reduction might be achieved by using different matrices, also with impacts on transmitter and receiver complexities.

TABLE IV  
FINAL COMPARISONS AMONG ALL PRESENTED SCHEMES IN TERMS OF THE MAIN METRICS.

	PAPR	Error-floor (SER)	Complexity		Explicit Information
			Tx	Rx	
OFDM	High	Moderate	Very low	Very low	No
WHT-OFDM	Moderate	High	Low	Low	No
SLM-WHT-OFDM	Low	Low	High	Low	Yes
SLM-WHT-WEI	Low	Low	High	High	No
DWHT	High	Moderate	Low	Low	No
SLM-DWHT-OFDM	Very Low	Very Low	Very High	Moderate	Yes

ACKNOWLEDGMENT

The authors would like to thanks the Prof. Christian Oberli for their valuable comments.

This work was partially supported by Finep, with resources from Funttel, Grant No. 01.14.0231.00, under the Radio-communication Reference Center (Centro de Referência em Radiocomunicações - CRR) project of the National Institute of Telecommunications (Instituto Nacional de Telecomunicações - Inatel) and CPqD - Brazil.

REFERENCES

[1] A. R. Bahai and B. R. Saltzberg, *Multi-Carrier Digital Communications: Theory and Applications of OFDM*. Plenum Publishing Co., 1999, doi: 10.1007/b99321.

[2] E. Charfi, L. Chaari, and L. Kamoun, "PHY/MAC enhancements and QoS mechanisms for very high throughput WLANs: A survey," *IEEE Communications Surveys Tutorials*, vol. 15, no. 4, pp. 1714–1735, April 2013, doi: 10.1109/SURV.2013.013013.00084.

[3] U. Reimers, "Digital video broadcasting," *IEEE Communications Magazine*, vol. 36, no. 6, pp. 104–110, June 1998, doi: 10.1109/35.685371.

[4] M. Takada and M. Saito, "Transmission system for ISDB-T," *Proceedings of the IEEE*, vol. 94, no. 1, pp. 251–256, January 2006, doi: 10.1109/JPROC.2005.859692.

[5] V. Stencel, A. Muller, and P. Frank, "LTE advanced; a further evolutionary step for next generation mobile networks," in *Proceedings of 20th International Conference Radioelektronika*, April 2010, pp. 19–21, doi: 10.1109/RADIOELEK.2010.5478548.

[6] S. Ahmadi, "An overview of next-generation mobile Wi-MAX technology," *IEEE Communications Magazine*, vol. 47, no. 6, pp. 84–98, June 2009, doi: 10.1109/MCOM.2009.5116805.

[7] C.-W. Pyo, X. Zhang, C. Song, M.-T. Zhou, and H. Harada, "A new standard activity in IEEE 802.22 wireless regional area networks: Enhancement for broadband services and monitoring applications in TV whitespace," in *Proceedings of the 15th International Symposium on Wireless Personal Multimedia Communications (WPMC)*, September 2012, pp. 108–112.

[8] D. Jiang and L. Delgrossi, "IEEE 802.11p: Towards an international standard for wireless access in vehicular environments," in *Proceedings of the IEEE Vehicular Technology Conference (VTC)*, May 2008, pp. 2036–2040, doi: 10.1109/VETECS.2008.458.

[9] G. Wunder and *et al.*, "5G NOW: non-orthogonal, asynchronous waveforms for future mobile applications," *IEEE Communications Magazine*, vol. 52, no. 2, pp. 97–105, February 2014, doi: 10.1109/MCOM.2014.6736749.

[10] R. v. Nee and R. Prasad, *OFDM for Wireless Multimedia Communications*, 1st ed. Norwood, MA, USA: Artech House, Inc., 2000.

[11] M. Ahmed, S. Boussakta, B. Sharif, and C. Tsimenidis, "OFDM based on low complexity transform to increase multipath resilience and reduce PAPR," *IEEE Transactions on Signal Processing*, vol. 59, no. 12, pp. 5994–6007, December 2011, doi: 10.1109/TSP.2011.2166551.

[12] A. Mallet, A. Anakabe, J. Sombrin, and R. Rodriguez, "Multipoint-amplifier-based architecture versus classical architecture for space telecommunication payloads," *IEEE Transactions on Microwave Theory and Techniques*, vol. 54, no. 12, pp. 4353–4361, December 2006, doi: 10.1109/TMTT.2006.885904.

[13] A. Bahai, M. Singh, A. Goldsmith, and B. Saltzberg, "A new approach for evaluating clipping distortion in multicarrier systems," *IEEE Journal on Selected Areas in Communications*, vol. 20, no. 5, pp. 1037–1046, June 2002, doi: 10.1109/JSAC.2002.1007384.

[14] L. Zhang, L.-L. Kuang, Z.-Y. Ni, and J.-H. Lu, "Performance evaluation for OFDM and SC-FDE systems with high power amplifier," in *Proceedings of the IET International Communication Conference on Wireless Mobile and Computing (CCWMC)*, December 2009, pp. 348–352, doi: 10.1049/cp.2009.1962.

[15] B. S. Chang, H. I. D. Monego, A. Munaretto, M. S. P. Fonseca, and R. D. Souza, "A simplified widely linear iterative equalizer for sc-fde systems," in *2017 Wireless Days*, March 2017, pp. 159–162, doi: 10.1109/WD.2017.7918134.

[16] F. Pancaldi, G. M. Vitetta, R. Kalbasi, N. Al-Dhahir, M. Uysal, and H. Mheidat, "Single-carrier frequency domain equalization," *IEEE Signal Processing Magazine*, vol. 25, no. 5, pp. 37–56, September 2008, doi: 10.1109/MSP.2008.926657.

[17] Y. Rahmatallah and S. Mohan, "Peak-to-average power ratio reduction in OFDM systems: A survey and taxonomy," *IEEE Communications Surveys Tutorials*, vol. 15, no. 4, pp. 1567–1592, April 2013, doi: 10.1109/SURV.2013.021313.00164.

[18] X. Zhu, H. Hu, and Y. Tang, "Descendent clipping and filtering for cubic metric reduction in OFDM systems," *Electronics Letters*, vol. 49, no. 9, pp. 599–600, April 2013, doi: 10.1049/el.2012.4350.

[19] X. Zhu, W. Pan, H. Li, and Y. Tang, "Simplified approach to optimized iterative clipping and filtering for PAPR reduction of OFDM signals," *IEEE Transactions on Communications*, vol. 61, no. 5, pp. 1891–1901, May 2013, doi: 10.1109/TCOMM.2013.021913.110867.

[20] M. Paredes Paredes and M. Fernandez-Getino Garcia, "Energy efficient peak power reduction in OFDM with amplitude predistortion aided by orthogonal pilots," *IEEE Transactions on Consumer Electronics*, vol. 59, no. 1, pp. 45–53, February 2013, doi: 10.1109/TCE.2013.6490240.

[21] M. Gay, A. Lampe, and M. Breiling, "An adaptive PAPR reduction scheme for OFDM using SLM with clipping at the transmitter, and sparse reconstruction at the receiver," in *Proceedings of the IEEE China Summit International Conference on Signal and Information Processing (ChinaSIP)*, July 2014, pp. 678–682, doi: 10.1109/ChinaSIP.2014.6889330.

[22] M. Hu, Y. Li, W. Wang, and H. Zhang, "A piecewise linear companding transform for PAPR reduction of OFDM signals with companding distortion mitigation," *IEEE Transactions on Broadcasting*, vol. 60, no. 3, pp. 532–539, September 2014, doi: 10.1109/TBC.2014.2339531.

[23] Y. Wang, J. Ge, L. Wang, J. Li, and B. Ai, "Nonlinear companding transform for reduction of peak-to-average power ratio in OFDM systems," *IEEE Transactions on Broadcasting*, vol. 59, no. 2, pp. 369–375, June 2013, doi: 10.1109/TBC.2012.2219252.

[24] J. Xiao, J. Yu, X. Li, Q. Tang, H. Chen, F. Li, Z. Cao, and L. Chen, "Hadamard transform combined with companding transform technique for PAPR reduction in an optical direct-detection OFDM system," *IEEE Journal of Optical Communications and Networking*, vol. 4, no. 10, pp. 709–714, October 2012, doi: 10.1364/JOCN.4.000709.

[25] P. Varahram and B. Ali, "A crest factor reduction scheme based on recursive optimum frequency domain matrix," *IEEE Transactions on Consumer Electronics*, vol. 60, no. 2, pp. 179–183, May 2014, doi: 10.1109/TCE.2014.6851991.

[26] S. Adegbite, S. McMeekin, and B. Stewart, "Low-complexity data decoding using binary phase detection in SLM-OFDM systems," *Electronics Letters*, vol. 50, no. 7, pp. 560–562, March 2014, doi: 10.1049/el.2013.4030.

[27] N. Singh, A. Bhadu, and A. Kumar, "Combined SLM and tone reservation for PAPR reduction in OFDM systems," in *Proceeding of the Confluence 2013: The Next Generation Information Technology Summit*, September 2013, pp. 274–277, doi: 10.1049/cp.2013.2327.

[28] S. Meymanatabadi, J. Niya, and B. Tazehkand, "Multiple recursive generator-based method for peak-to-average power ratio reduction in selected mapping without side information," *China Communications*, vol. 10, no. 8, pp. 68–76, August 2013, doi: 10.1109/CC.2013.6633746.

- [29] V. Sudha and D. Sriram Kumar, "PAPR reduction of OFDM system using PTS method with different modulation techniques," in *Proceeding of the International Conference on Electronics and Communication Systems (ICECS)*, February 2014, pp. 1–5, doi: 10.1109/ECS.2014.6892642.
- [30] E. Kalaiselvan, P. Elavarasan, and G. Nagarajan, "PAPR reduction of OFDM signals using pseudo random PTS without side information," in *Proceeding of the International Conference on Communications and Signal Processing (ICCS)*, April 2013, pp. 29–33, doi: 10.1109/iccs.2013.6577008.
- [31] S. Khademi and A. van der Veen, "Constant modulus algorithm for peak-to-average power ratio (PAPR) reduction in MIMO OFDM/A," *IEEE Signal Processing Letters*, vol. 20, no. 5, pp. 531–534, May 2013, doi: 10.1109/LSP.2013.2254114.
- [32] M. Gouda and M. Hussien, "Partial transmit sequence PAPR reduction method for LTE OFDM systems," in *Proceedings of the 4th International Conference on Intelligent Systems Modelling Simulation (ISMS)*, January 2013, pp. 507–512, doi: 10.1109/ISMS.2013.78.
- [33] H.-L. Hung and Y.-F. Huang, "Peak-to-average power ratio reduction in orthogonal frequency division multiplexing system using differential evolution-based partial transmit sequences scheme," *IET Communications*, vol. 6, no. 11, pp. 1483–1488, July 2012, doi: 10.1049/iet-com.2010.0997.
- [34] Z. Dlugaszewski and K. Wesolowski, "WHT/OFDM - an improved OFDM transmission method for selective fading channels," in *Proceedings of the Symposium on Communications and Vehicular Technology (SCVT)*, 2000, pp. 144–149, doi: 10.1109/SCVT.2000.923353.
- [35] S. Wang, S. Zhu, and G. Zhang, "A Walsh-Hadamard coded spectral efficient full frequency diversity OFDM system," *IEEE Transactions on Communications*, vol. 58, no. 1, pp. 28–34, January 2010, doi: 10.1109/TCOMM.2010.01.070605.
- [36] M. Al-Attraqchi, S. Boussakta, and S. Le-Goff, "An enhanced OFDM/OQAM system exploiting Walsh-Hadamard transform," in *Proceedings of the 73rd Vehicular Technology Conference (VTC Spring)*, May 2011, pp. 1–5, doi: 10.1109/VETECS.2011.5956311.
- [37] T. Su and F. Yu, "A family of fast Hadamard Fourier transform algorithms," *IEEE Signal Processing Letters*, vol. 19, no. 9, pp. 583–586, September 2012, doi: 10.1109/LSP.2012.2207452.
- [38] S. Ghosh, S. Talapatra, S. Maity, and H. Rahaman, "A novel VLSI architecture for Walsh-Hadamard transform," in *Proceedings of the 2nd Asia Symposium on Quality Electronic Design (ASQED)*, August 2010, pp. 146–150, doi: 10.1109/ASQED.2010.5548230.
- [39] L. Mendes and R. Baldini Filho, "Performance of WHT-STC-OFDM in mobile frequency selective channel," *Proceedings of the International Telecommunication Symposium (ITS)*, March 2010.
- [40] S. Mohammady, R. Sidek, P. Varahram, M. Hamidon, and N. Sulaiman, "Study of PAPR reduction methods in OFDM systems," in *Proceeding of the 13th International Conference on Advanced Communication Technology (ICTACT)*, February 2011, pp. 127–130.
- [41] L. Nadal, M. Svaluto Moreolo, J. Fabrega, and G. Junyent, "Comparison of peak power reduction techniques in optical OFDM systems based on FFT and FHT," in *Proceedings of the 13th International Conference on Transparent Optical Networks (ICTON)*, June 2011, pp. 1–4, doi: 10.1109/ICTON.2011.5971035.
- [42] I. Baig and V. Jeoti, "PAPR analysis of DHT-precoded OFDM system for M-QAM," in *Proceedings of the International Conference on Intelligent and Advanced Systems (ICIAS)*, June 2010, pp. 1–4, doi: 10.1109/ICIAS.2010.5716195.
- [43] —, "PAPR reduction in OFDM systems: Zadoff-Chu matrix transform based pre/post-coding techniques," in *Proceedings of the 2nd International Conference on Computational Intelligence, Communication Systems and Networks (CICSyN)*, July 2010, pp. 373–377, doi: 10.1109/CICSyN.2010.34.
- [44] L. L. Mendes, G. P. Aquino, and L. S. Resende, "Double Walsh-Hadamard Transform OFDM system - invited paper," *Especial Edición of Revista Telecomunicações*, vol. 15, no. 02, pp. 48–54, October 2013.
- [45] G. P. Aquino, L. L. Mendes, and L. S. Resende, "Melhoria da técnica de redução da PAPR baseada na transformada de Walsh-Hadamard," in *Proceedings of 30th Simpósio Brasileiro de Telecomunicações (SBrT)*, vol. 1, 2012, pp. 430–433.
- [46] G. P. Aquino, L. L. Mendes, and T. C. Pimenta, "Esquema para redução de PAPR em sistemas OFDM empregando as técnicas SLM e Double WHT," in *Proceedings of 31st Simpósio Brasileiro de Telecomunicações (SBrT)*, 2013, doi: 10.14209/sbrt.2013.133.
- [47] H. Ochiai and H. Imai, "On the distribution of the peak-to-average power ratio in OFDM signals," *IEEE Transactions on Communications*, vol. 49, no. 2, pp. 282–289, February 2001, doi: 10.1109/26.905885.
- [48] L. Hanzo, W. T. Webb, and T. Keller, *Single- and Multi-carrier Quadrature Amplitude Modulation: Principles and Applications for Personal Communications, WLANs and Broadcasting*, 2nd ed. London: IEEE Press, and John Wiley & Sons, 1999.
- [49] R. van Nee and A. de Wild, "Reducing the peak-to-average power ratio of OFDM," in *Proceeding of the 48th IEEE Vehicular Technology Conference (VTC)*, vol. 3, May 1998, pp. 2072–2076 vol.3, doi: 10.1109/VETEC.1998.686121.
- [50] C. C. Cadenas, J. R. Tosina, and M. J. Ayora, "Volterra behavioral model for wideband RF amplifiers," *IEEE Transactions on Microwave Theory and Techniques*, vol. 55, no. 3, pp. 449–457, March 2007, doi: 10.1109/TMTT.2006.890514.
- [51] S. C.ripps, *Advanced Techniques in RF Power Amplifier Design*. Norwood, MA: Artech House, 2002.
- [52] C. Rapp, "Effects of HPA-nonlinearity on a 4-DPSK/OFDM-signal for a digital sound broadcasting signal," in *Proceeding of the 2nd European Conference in Satellite Communications*, October 1991, pp. 179–184.
- [53] S. S. Agaian, H. Sarukhanyan, K. Egiastian, and J. Astola, *Hadamard transforms*. Bellingham, Washington, USA: SPIE press books, 2011, doi: 10.1117/3.890094. [Online]. Available: <http://opac.inria.fr/record=b1133616>
- [54] M. Park, H. Jun, J. Cho, N. Cho, D. Hong, and C. Kang, "PAPR reduction in OFDM transmission using Hadamard transform," in *Proceedings of the IEEE International Conference on Communications (ICC)*, 2000, pp. 430–433, doi: 10.1109/ICC.2000.853355.
- [55] C. Tellambura, "Upper bound on peak factor of N-multiple carriers," *Electronics Letters*, vol. 33, no. 19, pp. 1608–1609, September 1997, doi: 10.1049/el:19971069.
- [56] 3rd Generation Partnership Project, "3GPP TS 36.101, Technical Specification Group Radio Access Network; User Equipment (UE) Radio Transmission and Reception (Release 11)," 3rd Generation Partnership Project, Tech. Rep., 2014.
- [57] A. Trimeche, N. Boukid, A. Sakly, and A. Mtibaa, "Performance analysis of ZF and MMSE equalizers for MIMO systems," in *Proceedings of the 7th International Conference on Design Technology of Integrated Systems in Nanoscale Era*, May 2012, pp. 1–6, doi: 10.1109/DTIS.2012.6232979.
- [58] L. Resende, J. Romano, and M. Bellanger, "Split Wiener filtering with application in adaptive systems," *IEEE Transactions on Signal Processing*, vol. 52, no. 3, pp. 636–644, March 2004, doi: 10.1109/TSP.2003.822351.



**Guilherme Pedro Aquino** received the M.Sc. degree in telecommunications engineering from Instituto Nacional de Telecomunicações (Inatel), Brazil, and currently is a student of Doctor in Electrical Engineer degree from Universidade Federal de Itajubá, UNIFEI, Brazil. Since 2010 he is a professor and researcher at Inatel. His main research interests lie in the study of the non-orthogonal multiple access schemes and cooperative spectrum sensing techniques for cognitive radio applications.



**Luciano Leonel Mendes** received the B.Sc. and M.Sc. in Electrical Engineer from Inatel, Brazil in 2001 and 2003, respectively. In 2007 he received the Doctor in Electrical Engineer degree from Unicamp, Brazil. Since 2001 he is a professor at Inatel, Brazil. He has coordinated the Master Program at Inatel and several research projects funded by FAPEMIG, FINEP and BNDES. He has been a visiting researcher at Vodafone Chair Mobile Communications Systems at the TU Dresden between 2013 and 2015. His main area of research is waveforms for 5G networks and future mobile communication systems.